

SD83-BMDSCOM-2682

# Technical Report

## RADOME ANALYSIS

October 1983

AD A136805  
DTIC FILE COPY

THE VIEWS, OPINIONS, AND/OR FINDINGS CONTAINED IN THIS REPORT ARE THOSE OF THE AUTHOR(S) AND SHOULD NOT BE CONSTRUED AS AN OFFICIAL DEPARTMENT OF THE ARMY POSITION, POLICY, OR DECISION, UNLESS SO DESIGNATED BY OTHER OFFICIAL DOCUMENTATION.

DTIC  
ELECTE  
S JAN 13 1984 D  
D



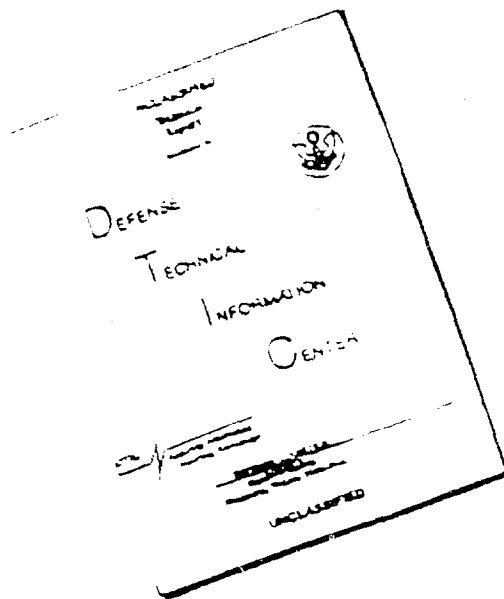
 **TELEDYNE  
BROWN ENGINEERING**

Cummings Research Park • Huntsville, Alabama 35807

**DISTRIBUTION STATEMENT A**  
Approved for public release;  
Distribution Unlimited

84 01 12 080

# DISCLAIMER NOTICE



THIS DOCUMENT IS BEST QUALITY AVAILABLE. THE COPY FURNISHED TO DTIC CONTAINED A SIGNIFICANT NUMBER OF PAGES WHICH DO NOT REPRODUCE LEGIBLY.

Accession For	
NTIS GRA&I	<input checked="" type="checkbox"/>
DTIC TAB	<input type="checkbox"/>
Unannounced	<input type="checkbox"/>
Justification	
By	
Distribution/	
Availability Codes	
Dist	Avail and/or Special
A/1	

Technical Report  
SD83-BMDSOM-2682

RADOME ANALYSIS

By

T. S. Pendergrass

October 1983



Prepared For:

Department of the Army  
Ballistic Missile Defense Command  
Systems Technology Project Office  
Huntsville, Alabama

Contract No. DASG60-81-C-0109

Prepared By:

Applied Science Branch  
Systems Analysis Department  
Teledyne Brown Engineering  
Cumings Research Park  
Huntsville, Alabama 35807

**DISTRIBUTION STATEMENT A**  
Approved for public release;  
Distribution Unlimited

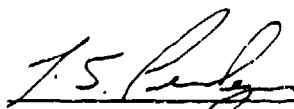
REPORT DOCUMENTATION PAGE		READ INSTRUCTIONS BEFORE COMPLETING FORM
1. REPORT NUMBER SD83-BMDSCOM-2682	2. GOVT ACCESSION NO. AD-A136 805	3. RECIPIENT'S CATALOG NUMBER
4. TITLE (and Subtitle) Radome Analysis	5. TYPE OF REPORT & PERIOD COVERED Technical Report June - August 1983	
	6. PERFORMING ORG. REPORT NUMBER SD83-BMDSCOM-2682	
7. AUTHOR(s) T. S. Pendergrass	8. CONTRACT OR GRANT NUMBER(s) DASG60-81-C-0109	
9. PERFORMING ORGANIZATION NAME AND ADDRESS Teledyne Brown Engineering Applied Science Branch Cummings Research Park Huntsville, Alabama 35807	10. PROGRAM ELEMENT, PROJECT, TASK AREA & WORK UNIT NUMBERS	
11. CONTROLLING OFFICE NAME AND ADDRESS Ballistic Missile Defense Command Huntsville, Alabama	12. REPORT DATE October 1983	
	13. NUMBER OF PAGES 38	
14. MONITORING AGENCY NAME & ADDRESS (if different from Controlling Office)	15. SECURITY CLASS. (of this report) Unclassified	
	15a. DECLASSIFICATION/DOWNGRADING SCHEDULE N/A since unclassified	
16. DISTRIBUTION STATEMENT (of this Report) Approved for public release, distribution unlimited		
17. DISTRIBUTION STATEMENT (of the abstract entered in Block 20, if different from Report)		
18. SUPPLEMENTARY NOTES This work was sponsored by the Ballistic Missile Defense Command under Contract Number DASG60-81-C-0109.		
19. KEY WORDS (Continue on reverse side if necessary and identify by block number) Radome Analysis                      Erosion Millimeter Wave Radome            Ablation Environmental Effects                Frequency Variation Thermal Effects		
20. ABSTRACT (Continue on reverse side if necessary and identify by block number) This report documents the usage and applications of the Ray Trace Formulation Radome Analysis Computer Program (RTFRACP) to the BMD ENNK Program. Methodology for applying the program to a generic millimeter wave radome is presented. Data is given to illustrate the effect of temperature, erosion, <del>ablation</del> and frequency variation on radome boresight error. <i>ablation</i>		

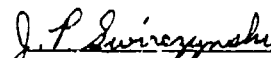
## Abstract

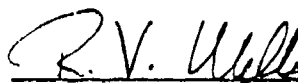
This Technical Report documents the results of an effort to acquire a capability in the area of radome analysis and design. The appropriate methodology has been developed to apply this analysis to the U.S. Army Ballistic Missile Defense (BMD) Endo-atmospheric Nonnuclear Kill (ENNK) Program.

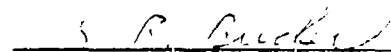
The following areas of study are included in this report: environmental effects (thermal, erosion, ablation) on radomes. Data is given for a generic millimeter wave radome that includes effects of temperature, erosion, and frequency variation on radome boresight error.

Approval:

  
\_\_\_\_\_  
T. S. Pendergrass

  
\_\_\_\_\_  
J. P. Swirczynski  
Section Manager,  
Tactical Systems Section

  
\_\_\_\_\_  
R. V. Wells  
Assistant Project Manager for  
ENNK Subsystems

  
\_\_\_\_\_  
K. R. Bucher  
Deputy Project Manager for  
Subsystem Design and Development

## Table of Contents

<u>Chapter</u>	<u>Title</u>	<u>Page</u>
1.	Introduction . . . . .	1
2.	Radome Design Theory and Analysis Methods . . . . .	2
2.1	The Missile Radome . . . . .	2
2.2	Radome Analysis Methods . . . . .	2
3.	Ray Trade Formulation Radome Analysis Computer Code (RTFRACP) . . . . .	5
3.1	General Description of RTFRACP Analysis . . . . .	5
3.2	RTFRACP Modifications . . . . .	12
4.	Applications of RTFRACP . . . . .	13
4.1	Introduction . . . . .	13
5.	Application of RTFRACP to MMW Radomes . . . . .	15
5.1	General . . . . .	15
5.2	Radome/Antenna Model . . . . .	15
5.3	Radome Materials . . . . .	15
5.4	Results. . . . .	19
6.	Conclusions and Recommendations . . . . .	34
7.	References . . . . .	35

## List of Figures

<u>Figure Number</u>	<u>Title</u>	<u>Page</u>
1.	Fast Receiving Method of Radome Analysis . . . . .	6
2.	Plane Wave Propagation Through an Infinite Plane Sheet . . . . .	7
3.	Radome/Antenna Configuration . . . . .	8
4.	Coordinate Systems Used in Radome Analysis . . . . .	10
5.	RTFRACP Coordinate Systems . . . . .	11
6.	Generic Millimeter Wave Radome . . . . .	16
7.	Radome/Antenna Scan Angle . . . . .	17
8.	Temperature Effects on Azimuth BSE-vs-Scan Angle . . . . .	20
9.	RTFRACP Azimuth and Elevation Scan Planes . . . . .	21
10.	Temperature Profile Across the Thickness of the Radome Wall . . . . .	19
11.	Temperature Effects on Elevation BSE-vs-Scan Angle . . . . .	23
12.	Model for Determining Temperature at 0°-20° Scan Angles . . . . .	24
13.	Temperature Along Radome Length . . . . .	25
14.	Temperature at 0°-20° Scan Angles . . . . .	26
15.	Temperature Effects on Azimuth BSE-vs-Scan Angle . . . . .	27
16.	Temperature Effects on Elevation BSE-vs-Scan Angle . . . . .	28
17.	Effect of Erosion on Azimuth BSE-vs-Scan Angle . . . . .	30
18.	Effect of Frequency Variation on Azimuth BSE-vs- Scan Angle . . . . .	32

List of Figures (continued) -

<u>Figure Number</u>	<u>Title</u>	<u>Page</u>
19.	Effect of Frequency Variations on Elevation BSE-vs-Scan Angle . . . . .	33

## List of Tables

<u>Table Number</u>	<u>Title</u>	<u>Page</u>
1.	Properties of Candidate Radome Materials . . . . .	18
2.	Temperature and Dielectric Properties at 0°-20° Scan Angles . . . . .	29

## I. INTRODUCTION

The purpose of this report is to document the results of an effort to acquire a capability in the area of radome analysis and design. Also, the appropriate methodology has been developed to apply this analytical tool to the U.S. Army Ballistic Missile Defense (BMD) Endo-atmospheric Non-Nuclear Kill (ENNK) Program.

To obtain the small miss distances required by the ENNK interceptor, guidance loop stability must be maintained even in the presence of homing guidance errors introduced by radome boresight error (BSE). This situation is further complicated by evidence that high performance ceramic radomes experience substantial increases in boresight error (BSE) and boresight error slope (BSES) as a result of the intense environments encountered. These environments include: aerodynamic heating and ablation caused by the hypersonic velocity of the interceptor, additional heating due to nuclear detonations, and material erosion due to flight through dust or rain.

This report documents the applications and usage of the Ray Trace Formulation Radome Analysis Computer Program (RTFRACP). Also, data for a generic millimeter wave radome is presented.

## 2. RADOME DESIGN THEORY AND ANALYSIS METHODS

### 2.1 The Missile Radome

The missile radome is a protective dielectric housing for microwave or millimeter wave antenna. The function of the radome is to protect the antenna from adverse environments while having an insignificant effect on the electrical performance of the enclosed antenna or antennas.

Radomes are generally designed using low-loss dielectrics of thickness on the order of the antenna wavelength. They are shaped to cover the antenna and conform to aerodynamic streamlining. A radome design is a quantitative description of the radome configuration and material composition. For a specific application, the radome shape and the materials are usually chosen to satisfy structural and environmental requirements. Within these constraints it is possible to choose the type of radome, i.e., whether the radome consists of a single homogenous shell or of several distinct layers. Then, with the frequencies specified, the electromagnetic design problem is to determine the thickness of the various layers, the materials (subject to environmental requirements), and variations in thickness to obtain useful values of quantities such as transmittance, sidelobe levels, and boresight error. The main result of a theoretical design procedure is a prediction of the transmittance, sidelobe levels, and boresight error. Then, by comparing the values for several distinct designs, an optimum design for a particular application can be chosen.

The fraction of energy transmitted through the radome is its transmittance. Boresight error is an apparent change in the angular position of a radar source or target. As a consequence of these effects, a radome can reduce both the accuracy in determining the angular position of a target and the range at which the target can be detected. In addition, a radome can change the sidelobe level of an antenna, which is a subsidiary maxima in the radiation pattern of the antenna.<sup>1,2</sup>

### 2.2 Radome Analysis Methods

The area of radome analysis is a complex and evolutionary discipline. The methods of analysis are constantly under refinement as can be seen from the following background information.

Until 1949 the only approach used to study tracking error in airborne radar systems was that of geometrical optics.<sup>3</sup> Kilcoyne refined this method and developed a two-dimensional ray tracing method for analyzing radomes which utilized the digital computer.<sup>4</sup> About the same time Kilcoyne presented his approach, a new method by Van Doeren was introduced.<sup>5</sup> Van Doeren's method used an integral equation to compute the fields inside the radome caused by an incident plane wave. Next, Tricoles formulated a three-dimensional method based upon Shelkunoff's induction and equivalence theorems.<sup>6</sup> Then Tavis described a three-dimensional ray tracing technique to find the fields on an equivalent aperture external to an axially symmetric radome.<sup>7</sup> Paris developed a three-dimensional radome analysis wherein the tangential fields on the outside surface of the radome due to the horn antenna radiating inside the radome could be found.<sup>8</sup> Wu and Rudduck described a three-dimensional method which used the plane wave spectrum representation to characterize the antenna.<sup>9</sup> Joy and Huddleston expanded on this concept and used the Fast Fourier Transform (FFT) to speed up the computer calculations when using the plane wave spectrum method.<sup>10</sup> Later, Chesnut combined the Wu and Rudduck program with the work of Paris to form a three-dimensional radome analysis method.<sup>11</sup> Huddleston developed a three-dimensional analysis method which uses a general formulation based on the Lorentz reciprocity theorem.<sup>12</sup> Siwiak, et. al., applied the reaction theorem to the analysis of a tangent ogive radome at x-band frequencies to determine boresight error.<sup>13</sup> Hayward, et. al., have compared the accuracies of two methods of analysis in the cases of large and small radomes to show that ray tracing does not accurately predict wavefront distortion in the case of small radomes.<sup>14</sup> Burks developed a ray tracing analysis which includes first-order reflections from the radome wall.<sup>15</sup> Kvam has applied the unimoment method to the solution of the radome problem.<sup>16</sup> It is apparent from this background that the development and refinement of accurate and efficient radome analysis computer codes will continue.

Today there are four primary approaches to radome analysis. These methods include the transmit formulation, the receive formulation, the plane wave spectra method, and the surface integration method. There are many variations of radome analysis, but they usually incorporate the use of one or more of these four primary approaches to the analysis.<sup>2</sup>

In this study, two radome analysis computer programs were investigated. Both codes were developed by G. K. Huddleston, H. L. Bassett, and J. M. Newton at the Georgia Institute of Technology.<sup>17</sup> The first computer code investigated was the Surface Integration Radome Analysis Computer Program (SIRACP). As the title implies, this code utilizes the surface integration approach to radome analysis. The second program, the Ray Trace Formulation Radome Analysis Computer Program (RTFRACP), utilizes the fast receive formulation as the approach to radome analysis.

It has been concluded that there is room for improvement in the predictive accuracies of radome analysis computer codes. This conclusion is especially true for the case of small antennas and radomes where the effects of antenna/radome interaction are not properly included. For the moderate sized radomes (the ENNK radome) the fast receive method (RTFRACP) is attractive because of the fast computational run time and reasonably accurate results.<sup>17</sup> The surface integration code (SiRACP) was still in the developmental stages when its documentation was released. However, it is clear that the applicability of the surface integration method would be restricted to small radomes because of the relatively long computation run times required (255 seconds per look angle for the surface integration method versus 35 seconds per look angle for the fast receive method). Based upon this information, the Ray Trace Formulation Radome Analysis Computer Program (RTFRACP) was selected for use in this study. (For further information see Reference 17).

### 3. RAY TRACE FORMULATION RADOME ANALYSIS COMPUTER PROGRAM

#### (RTFRACP)

##### 3.1 General Description of RTFRACP Analysis

RTFRACP is a Fortran computer used to analyze the effects of a tangent ogive radome on the performance of a monopulse aperture antenna. This program uses a receiving formulation based upon the Lorentz reciprocity theorem.<sup>17</sup>

A plane wave of either linear or circular polarization (selected by the user) is assumed incident on the outside of the radome. This wave is represented by a system of parallel rays (see Figure 1).<sup>17</sup> There is one ray for each sample data point in the antenna aperture inside the radome. Each ray is traced from the point of incidence on the outside surface to the corresponding aperture point. The incident electric and magnetic fields  $\underline{E}_i$ ,  $\underline{H}_i$  associated with each ray are biased by the flat plate transmission coefficients  $T_{||}$ ,  $T_{\perp}$  as determined by the unit normal vector  $\hat{n}$ , the direction of propagation  $\hat{k}$ , and the dielectric properties (dielectric constant and loss tangent) of the radome wall (see Figure 2).<sup>17</sup> The biased incident fields  $\underline{E}_j$ ,  $\underline{H}_j$  at each aperture point are then used to obtain the complex voltage response  $V_r$  of the antenna from the following integral.<sup>17</sup>

$$V_r = C \iint_S (\underline{E}_T \times \underline{H}_i - \underline{E}_i \times \underline{H}_T) \cdot \hat{Z} dx dy \quad (1)$$

$\underline{E}_T$ ,  $\underline{H}_T$  are the aperture fields when the antenna is transmitting,  $C$  is a complex constant, and  $\hat{Z}$  is the unit normal vector to the aperture ( $xy$ ) plane.

RTFRACP, as implemented on the SSS computer facility, allows for only one radome shape, i.e., the tangent ogive. For this shape, the user can vary the length, diameter, and fineness ratio (see Figure 3).<sup>17</sup> The fineness ratio is simply the ratio of length to diameter. This code allows the analysis of both monolithic and multilayer wall configurations with allowance for the analysis of a five layer radome. Provisions can be made in the code to allow for a metal tip on the radome. The effect of such a tip is blockage of the aperture.

The geometry subroutines provide three separate coordinate systems (Figures 4,5)<sup>17</sup> and the point and vector transformations among them. One

ILLUSTRATION OF THE FAST RECEIVING METHOD OF RADOME ANALYSIS

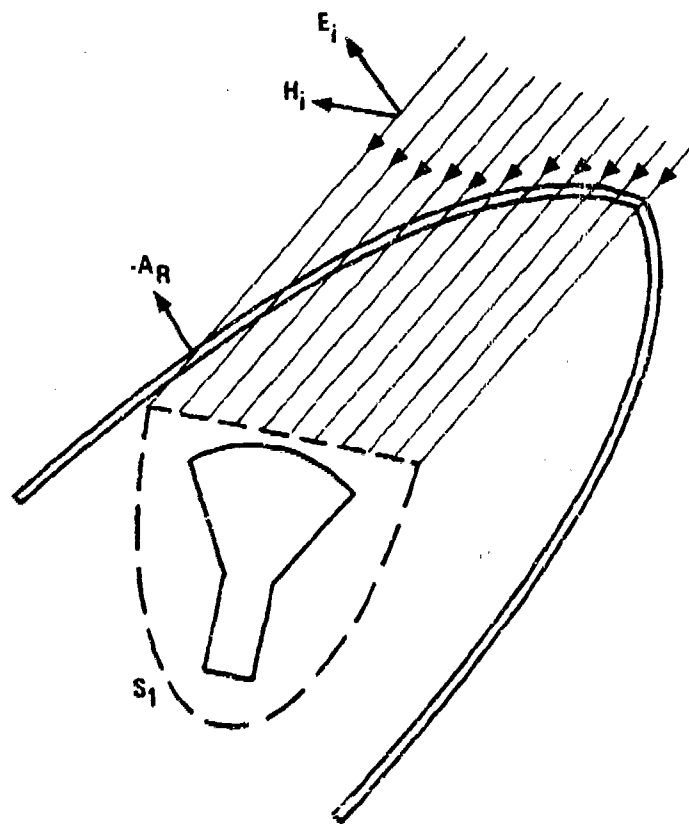


FIGURE 1. FAST RECEIVING METHOD OF RADOME ANALYSIS

PLANE WAVE PROPAGATION THROUGH AN INFINITE PLANE SHEET

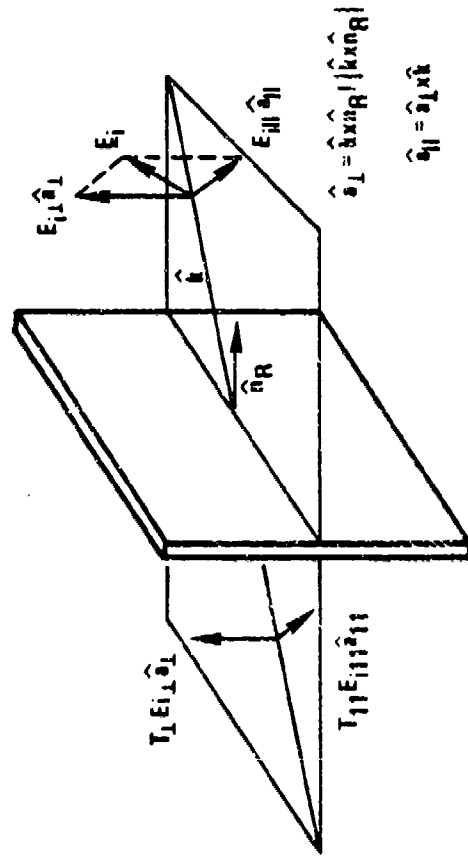


FIGURE 2. PLANE WAVE PROPAGATION THROUGH AN INFINITE PLANE SHEET

136-10

### RADOME/ANTENNA CONFIGURATION

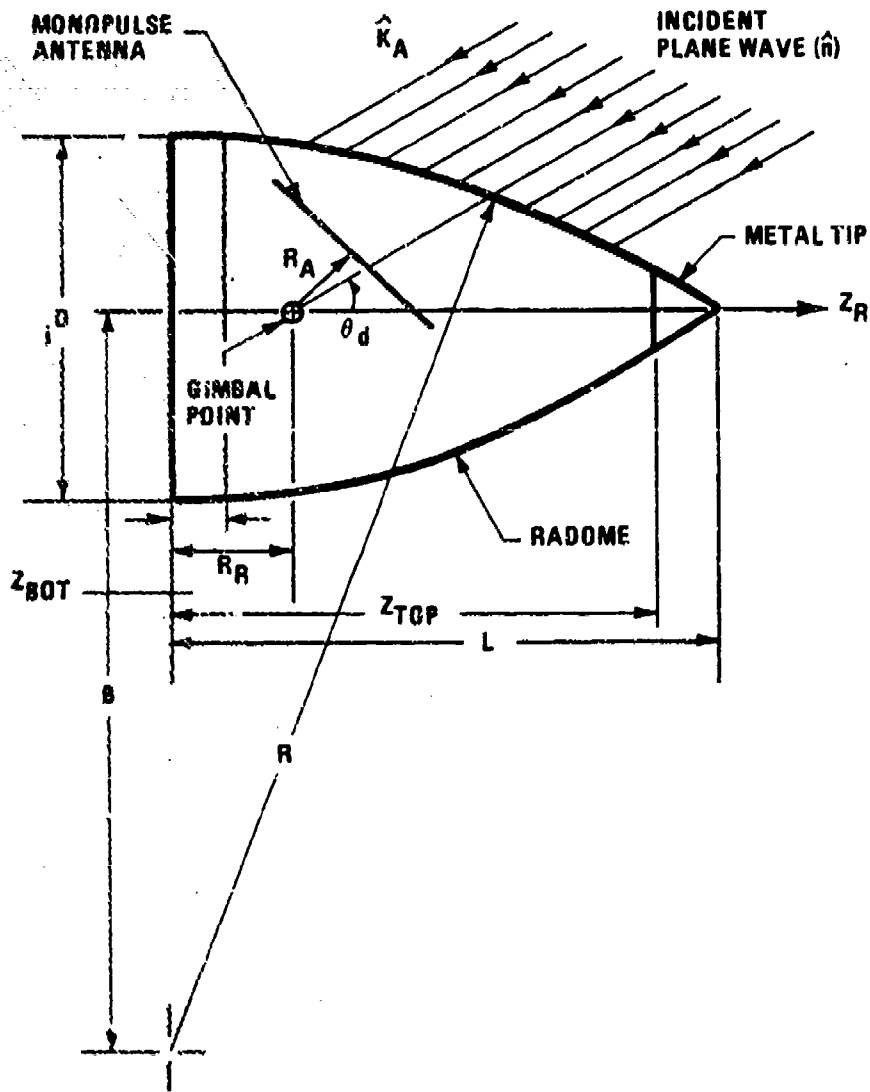


FIGURE 3. RADOME/ANTENNA CONFIGURATION

reference coordinate system orients the radome/antenna combination with respect to other objects. Separate coordinate systems are provided for both the antenna and radome. Pattern computations and boresight error computations are exercised and expressed in the antenna coordinate system.<sup>17</sup>

The subroutine used to characterize the antenna permits selection of various polarizations and two aperture distributions. A uniform, circular aperture distribution having vertical, horizontal, or circular (either left-hand or right-hand circular) polarizations is one combination. The second distribution which is available is a tapered rectangular distribution having vertical polarization similar to the flat plate antenna. This subroutine could easily be modified to accommodate other distributions, such as the rectangular aperture with cosine taper.<sup>17</sup>

For monopulse antennas, boresight error calculations are carried out by setting the first target return in a specified plane, at a few degrees within the true boresight error. This value is used as a "seed" by which the responses in the two different channels and the sum channel are computed and stored. Another set of responses for a target return 180° away from the first return is computed next. These two sets of data are used to construct a linear tracking model in the two orthogonal (azimuth and elevation) planes. The process is repeated until a null boresight is indicated. The boresight error is represented by true direction of arrival of the plane wave where a null boresight error is indicated.<sup>17</sup>

RTFRACP output data is given in the antenna coordinate system. These outputs include: (1) boresight error (mrad), (2) boresight error slope (deg/deg), (3) gain loss (db), and when selected as an additional output option, (4) principle plane patterns. These outputs are printed and can, also, be plotted using the CDC 7600 CALCOMP Plotter. The code also has an option to print intermediate results for debugging purposes.

The complete computer program consists of one main program and thirty-four subroutines. The core storage requirements for the program, including all library functions and system input/output routines, is approximately 46,000 decimal words.

COORDINATE SYSTEMS USED IN RADOME ANALYSIS

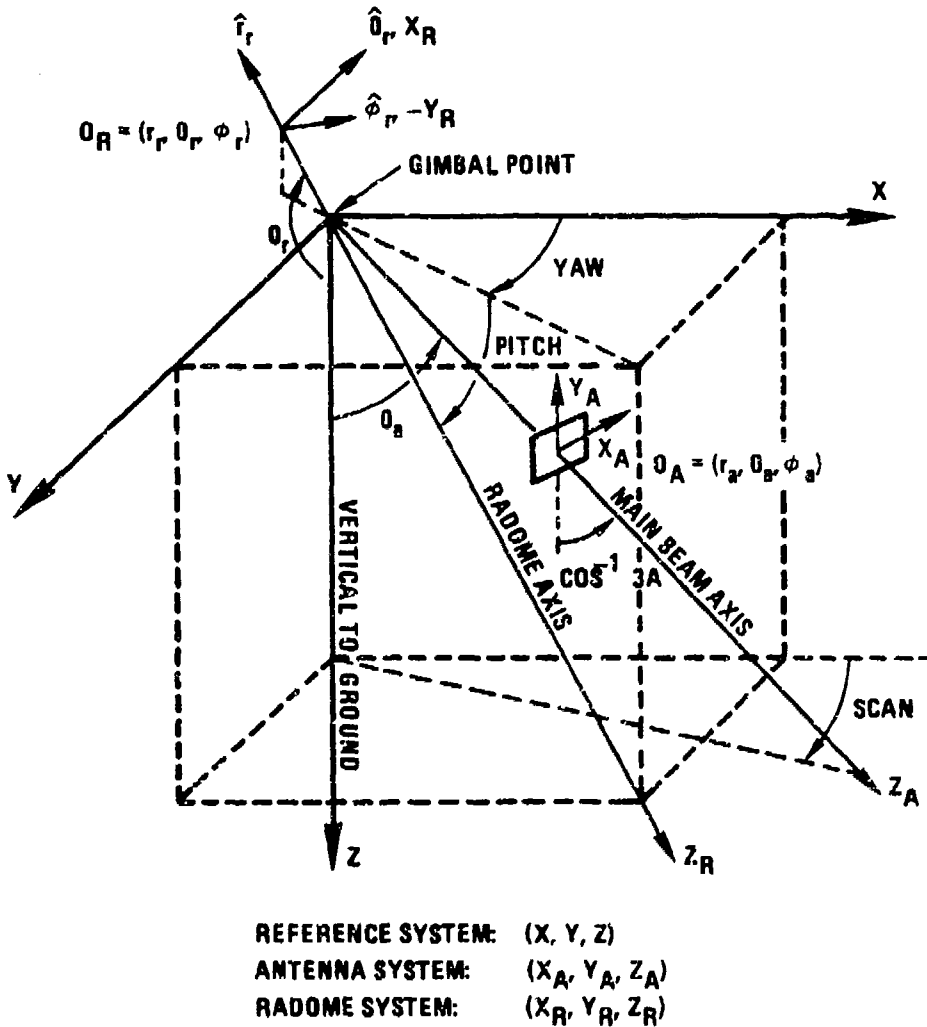
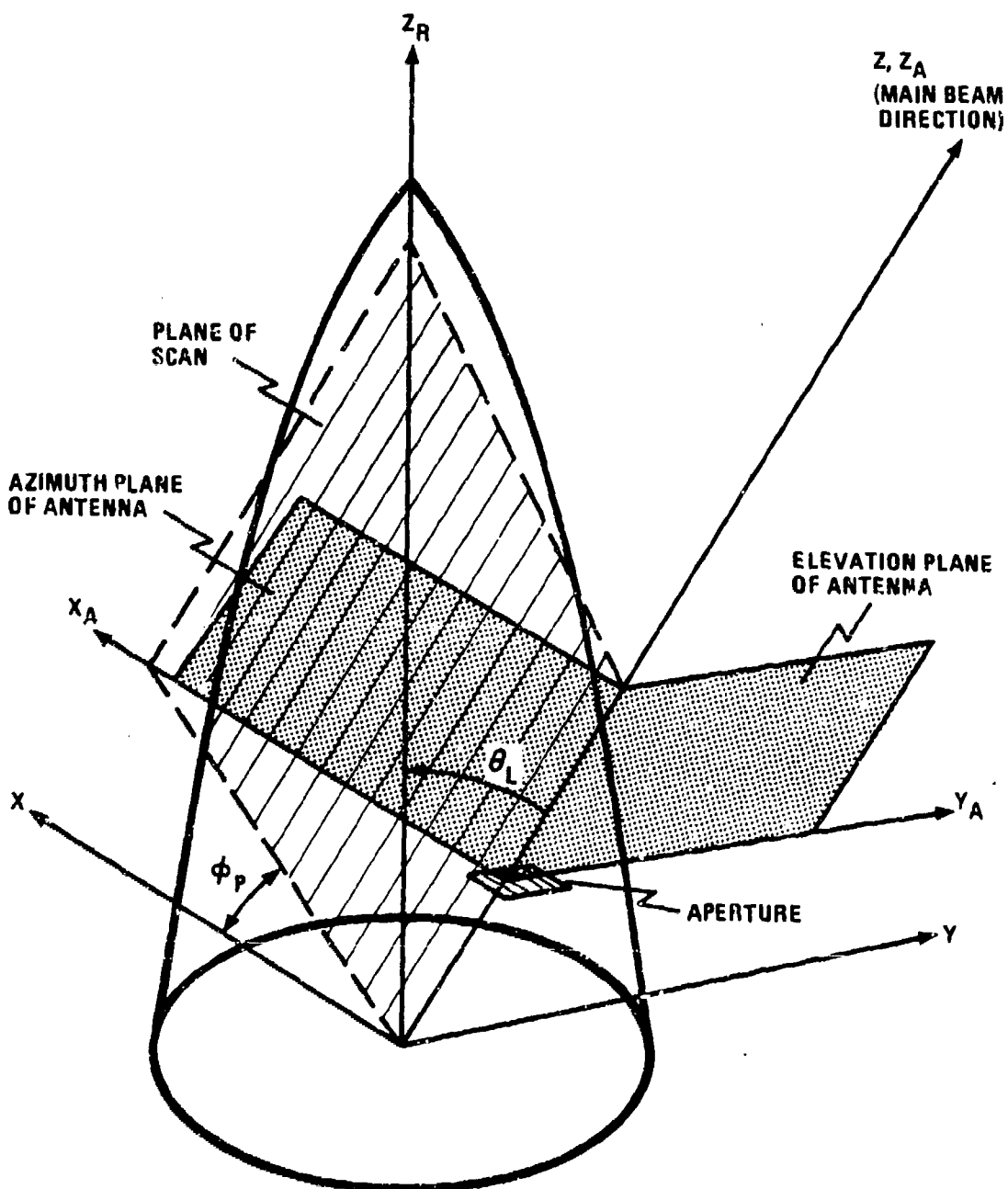


FIGURE 4. COORDINATE SYSTEMS USED IN RADOME ANALYSIS

RTFRACP COORDINATE SYSTEMS



$\phi_p$  = ANGLE OF SCAN PLANE —  $0^\circ$  AZIMUTH  
 $\theta_L$  = LOOK ANGLE                       $90^\circ$  ELEVATION

FIGURE 5. RTFRACP COORDINATE SYSTEMS

The time required to compute the transmitted and receiving patterns and aperture near fields and to execute the necessary CALCOMP commands for two dimensional plotting is approximately 35 seconds per look angle. Computation time is totally independent of the radome size but is dependent upon the number of samples used in the aperture (16 X 16 array). For this aperture spacing, boresight error (BSE), bore error slopes (BSES), and gain losses are computed in less than one second per look angle. These three parameters are normally the only outputs needed.

### 3.2 RTFRACP Modifications

RTFRACP adequately treats frequencies of less than 15 GHz with a 16 X 16 aperture distribution. For BMD ENNK applications (millimeter wavelength 35 GHz), a 16 X 16 aperture distribution is not adequate because of convergence problems. The spacing between the aperture grid points should be less than one wavelength apart. A 64 X 64 aperture distribution was selected which resulted in a 0.5 wavelength spacing between grid points for increased accuracy.

RTFRACP analysis with a 16 X 16 aperture grid pattern could be done on the CDC 7600 in small core memory. However, increasing the aperture grid pattern to a 64 X 64 array caused small core memory overflow. To alleviate this problem, modifications were made to the program. Many arguments were placed in Level 2 (large core memory). Arguments in Level 2 cannot be passed as arguments in subroutine call statements; they are passed in common statements. These changes increased compilation time from 5.6 seconds (16 X 16 grid) to 6.5 seconds (64 X 64 grid). The execution time for RTFRACP to calculate BSE, BSES and gain losses for this latter case is approximately 2.3 seconds per look angle.

## 4. APPLICATIONS OF RTFRACP

### 4.1 Introduction

In this section various applications and modeling techniques for RTFRACP will be discussed for millimeter wave radomes. Results of these modeling techniques will be shown. Applications of RTFRACP to radome design, material sensitivity analysis, and environmental effects will be included in this discussion. BSE results will be stressed as the major output of interest.

As mentioned in an earlier chapter, a radome design is a quantitative description of the radome configuration and composition. In the typical design process, a frequency of operation would be chosen, depending upon the system's mission and operating scenario. Next, the radome shape would be chosen based upon dimensional constraints and the desired aerodynamics. The choice of the radome materials would be based upon desired structural and electrical properties as well as environmental constraints. Based upon these data, it is possible to select the order of the radome wall. Then, with the frequency bandwidth specified, the next process is to determine the thickness and materials of the various layers. It should be realized that this design process is iterative, and all of the disciplines of design are interrelated.

RTFRACP is a design and analysis tool which can be used to determine the effect of a design change on a specific radome. This code can be used to evaluate the effects of a change in length, diameter, wall thickness, wall type, frequency of operation, seeker diameter, seeker location relative to the radome base, or polarization of the antenna. This eliminates the need for testing until the design is close to finalization.

RTFRACP can be used to study the effect of various environments (i.e., thermal, erosion, ablation) on radomes. Obviously, it is necessary in the design process to determine the environmental conditions that the radome will encounter. In hypersonic flight the radome will be heated due to the aerodynamic environment. Also, there may be nuclear detonations in the area which will also raise the temperature of the radome. For some materials, ablation may occur or even be enhanced due to the aerodynamic and nuclear environment. Erosion can occur in some materials due to abrasive environments

such as rain or dust. Each of these environments will have some effect upon radome performance, and the use of RTFRACP is an effective way to determine their impact on sensor performance without resorting to actual testing. Testing would not be totally eliminated through the use of this code, but the amount of testing should be greatly reduced.

## 5. APPLICATIONS OF RTFRACP TO MMW RADOMES

### 5.1 General

RTFRACP was modified to allow analysis of millimeter wave radomes (see Chapter 3.2) for BMD ENNK studies. This chapter will detail the analysis assumptions and modeling techniques used in this effort. Sample output and data is shown for a generic MMW radome design. An effort has been made to determine the increase in BSE as a result of elevated temperatures due to hypersonic flight. Results are also given to show an increase in BSE as a result of frequency bandwidth variations. Data is also given to show the effect of erosion on BSE.

### 5.2 Radome/Antenna Model

The radome/antenna geometry model used in the following discussion is illustrated in Figure 6. The radome has an outside base diameter of 14 inches, a length of 24 inches, a fineness ratio of 2.86, and the thickness of the radome wall is 0.122 inches. The fineness ratio in RTFRACP is used to set the outside radius of curvature of the radome. A fineness ratio of 2.86 corresponds to 118.0 inches for the outside radius of curvature for this particular radome. The monopulse antenna has a 12 inch diameter circular aperture with uniform illumination. The antenna scans from  $0^\circ$  to  $20^\circ$  as measured from the tip of the radome centered at the antenna gimbal point (see Figure 7). The distance from the base of the radome to the gimbal point of the antenna is 5.0 inches. The distance of the gimbal point to the aperture is 1.0 inches. The frequency of operation is 35 GHz.

### 5.3 Radome Materials

Candidate materials for hypersonic applications must be selected on the basis of good electrical characteristics and adequate aeromechanical strength in the  $2,000^\circ$  F temperature regime. Since organic materials are not suited to temperatures greater than  $450^\circ$  F, ceramics are the only viable candidates. The criteria used for the selection of acceptable wall materials is based on: (1) thermal shock indices of at least 1,000, (2) adequate mechanical strength properties to  $2,000^\circ$  F, (3) melt/decomposition temperatures above  $3,000^\circ$  F, (4) maximum material loss tangents of 0.10, (5) rain erosion resistance in the

# GENERIC MILLIMETER WAVE RADOME

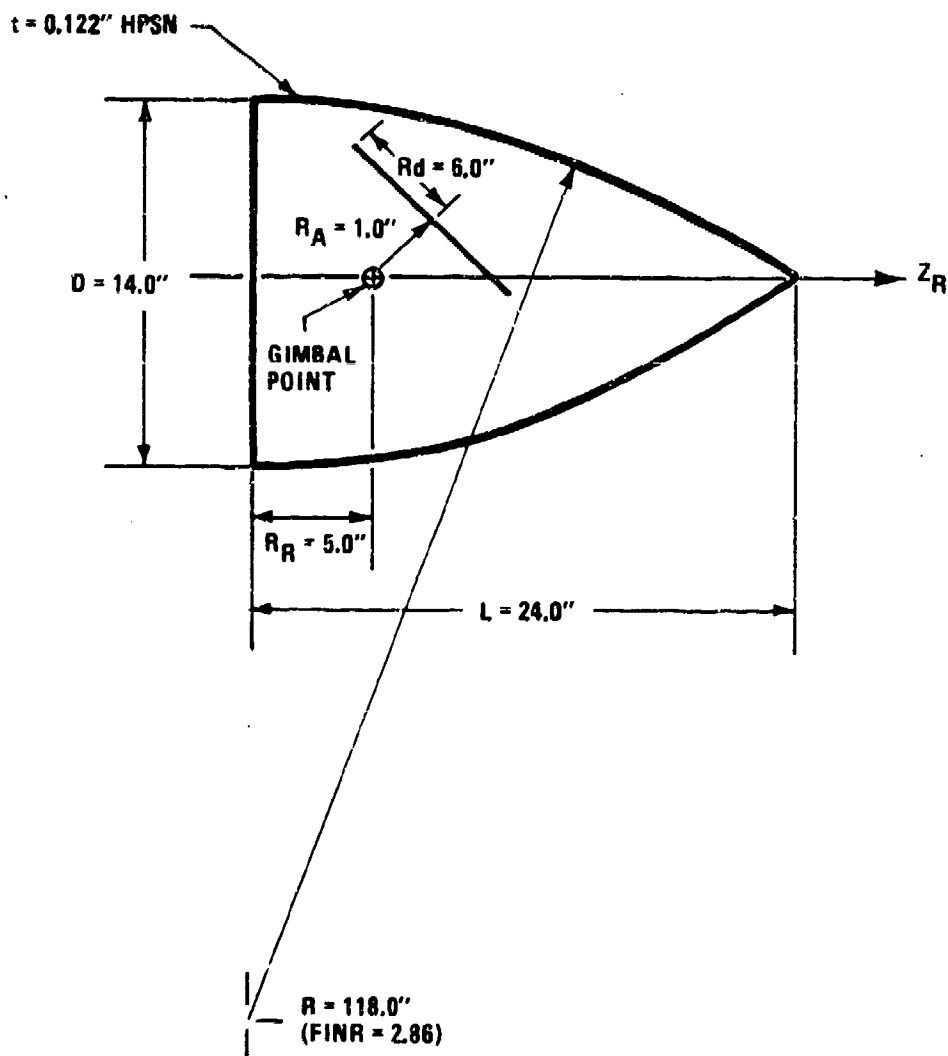


FIGURE 6. GENERIC MILLIMETER WAVE RADOME

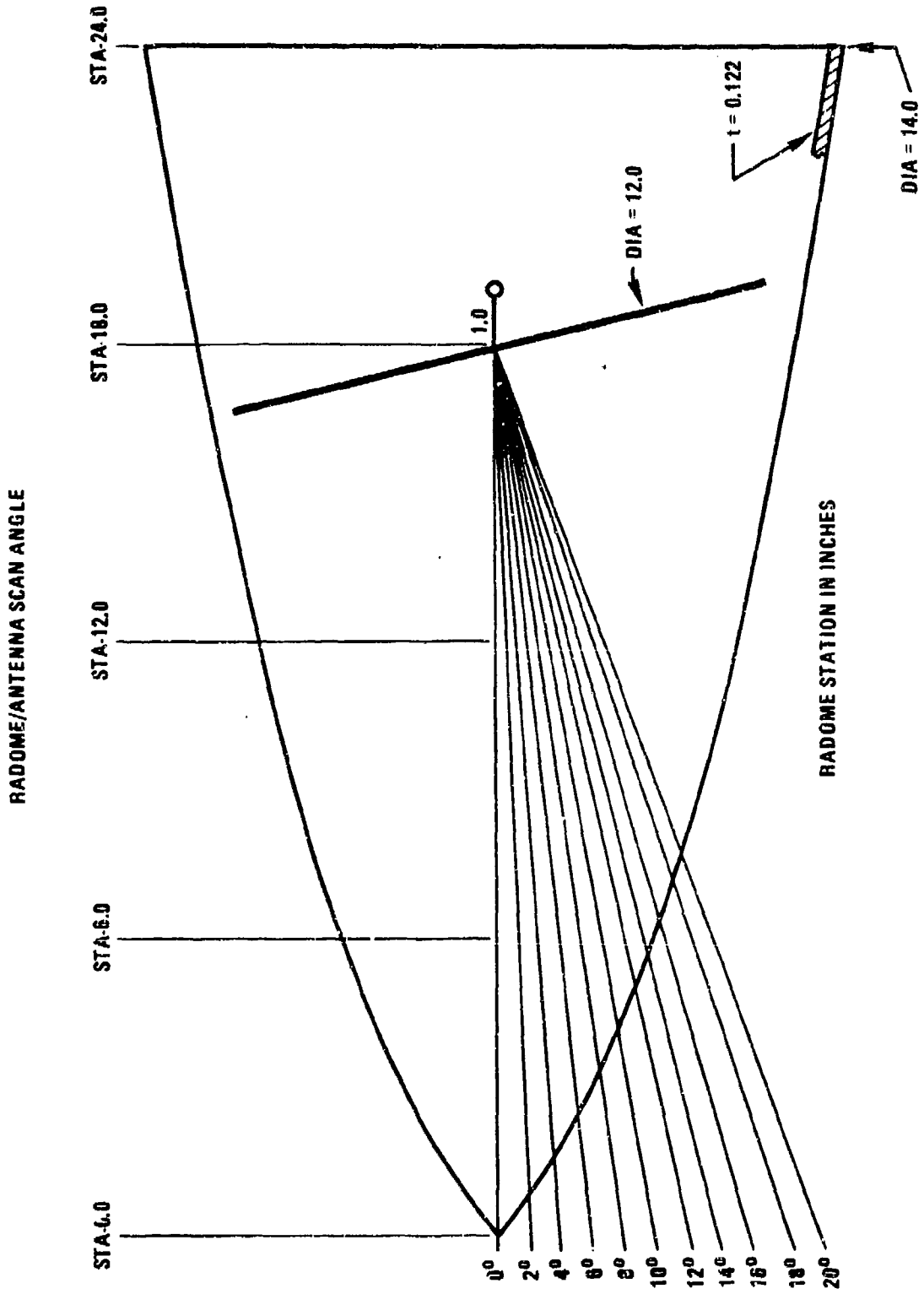


FIGURE 7. RADOME/ANTENNA SCAN ANGLE

hypersonic environment. Table I shows the properties of several candidate radome materials.

Table I. Properties of Candidate Radome Materials

<u>Property</u>	<u>SCFS</u>	<u>3-D Silica</u>	<u>HPSN</u>	<u>RSSN</u>	<u>BeO</u>
Melt temp. (F°)	3100	3100	3450	3400	4650
Thermal conductivity 10° (BTU/in-S-°F) 12	8.6	417	185	2778	
Flexural strength RT (ksi) - 2000°F	5 9	5 9	87-130 28-57	25	35-40 27
Poissons Ratio	.15	.17	.25	.25	.34
Modulus of elasticity (Mpsi)	4	3	15	14	
Coefficient of thermal expansion (10 <sup>-6</sup> /°F)	0.3	0.3	1.67	1.4	
Thermal shock index	4200	5550	1190		150
Dielectric constant*	3.4	3.2	8.5	5.6	6.64
Loss tangent*	.001	.004	.003	.002	.005
Rain erosion resistance	Fair	Good	High	High	Good
Cost	Low	High	High	Med.	High

\*RT

Studies of Martin Marietta Aerospace have indicated that the 50 Ksi tensile strength of hot pressed silicon nitride (HPSN) may permit the use of a half wave wall (N = 1 order) at 35 GHz.<sup>18</sup> This thickness corresponds to 0.127 inches. The use of materials with lower mechanical strength properties is feasible; however, higher wall orders are required, and this would increase BSE.

Since this study is not a materials optimization study, one material was chosen. That material is Type 147A(3553-1) HPSN (1% MgO sintering aid).<sup>19</sup> Kozakoff has developed curve fit dielectric models for the material.<sup>20</sup> The dielectric constant and loss targets are given as:

$$\text{Dielectric Constant} = 8.17 + 0.00016T + 0.11 \exp \left( \frac{2}{(T - 1472)/1440} \right)$$

and,

$$\text{Loss Tangent} = 0.007 + 0.0002 \exp(0.00165T). \quad (3)$$

These models are valid to 3,000°F at 35 GHz.<sup>20</sup>

#### 5.4 Results

Figure 8 is a plot of azimuthal boresight error (BSE) versus scan angle. BSE is given in milliradians. Scan angle is defined as the angle in degrees from the nose tip of the radome (Figure 7). Azimuth angle corresponds to yaw, and elevation corresponds to pitch as shown in Figure 9.

Figure 8 shows the dependency of BSE to temperature variations (200° F to 1,400° F). At 8 degrees scan angle, the BSE is approximately - 0.2 mrad at 200° F and - 6.3 mrad at 1,400° F. This corresponds to a 6.5 mrad change in BSE. It was assumed in these calculations that the radome temperature is constant across the thickness of the wall as well as along the length. Note the curve between 1000° F and 1200° F. This represents the results of a calculation that assumes a linear temperature distribution through the wall of the radome (see Figure 10). The temperature distribution was modeled as a five layer material where each layer has different dielectric properties corresponding to the average bulk temperature of each layer (Figure 10).

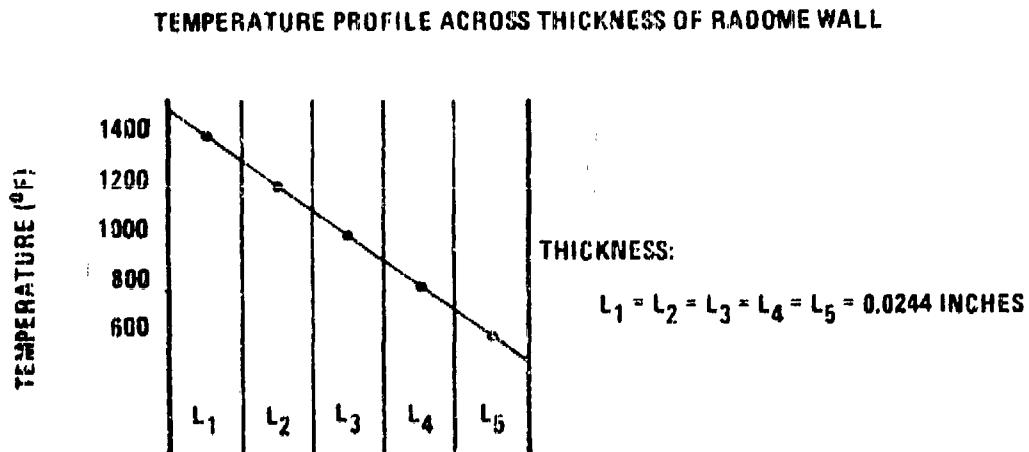


Figure 10. Temperature Profile Across Radome Wall

TEMPERATURE EFFECTS ON AZIMUTH BSE - VS. SCAN ANGLE  
 0° SCAN PLANE  
 HPSN 147E-5481-1

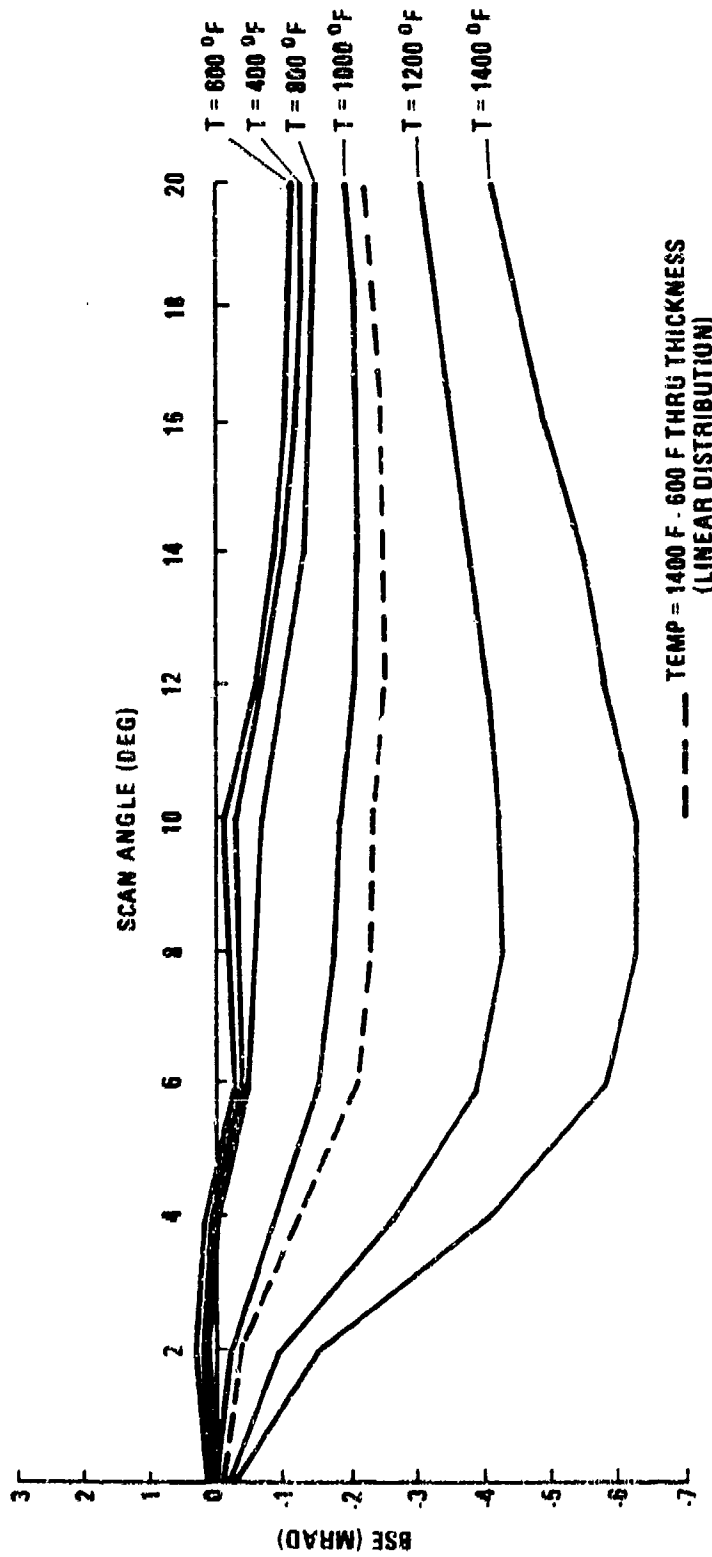
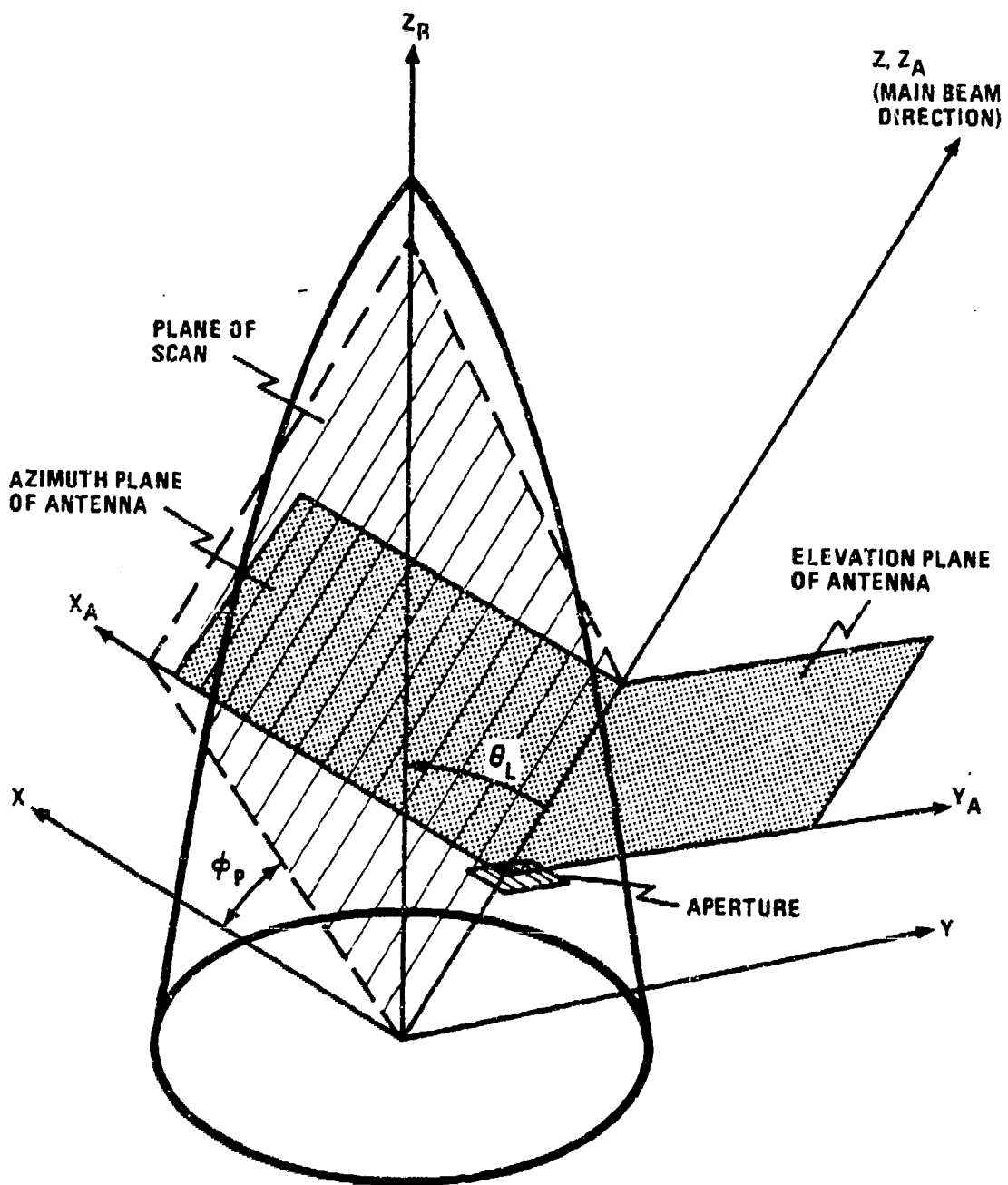


FIGURE 8. TEMPERATURE EFFECTS ON AZIMUTH BSE-VS-SCAN ANGLE

RTFRACP COORDINATE SYSTEMS



$\phi_p$  = ANGLE OF SCAN PLANE —  $0^\circ$  AZIMUTH  
 $\theta_L$  = LOOK ANGLE                     $90^\circ$  ELEVATION

FIGURE 9. RTFRACP AZIMUTH AND ELEVATION SCAN PLANES

Figure 11 illustrates the temperature dependence of elevation BSE as a function of scan angle. At 1400° F the maximum BSE is approximately 2.9 mrad at 8 degrees scan angle. At 200° F the maximum BSE is about -4.2 mrad at 6 degrees scan angle. The graph shows less BSE for 1000° F than for 200° F. The curve between 1000° F and 1200° F again represents the case where the wall is modeled with a linear temperature distribution between the inner and outer wall (Figure 10). It should be emphasized that the user can model practically any desired temperature distribution provided it can be done with 5 material layers or less.

Figure 12 shows a model developed to treat a longitudinal temperature variation similar to the actual flight environment. Radome station is defined as the distance from the tip of the radome in inches. The tip of the radome is 1400° F, the base is 600° F. By looking at scan angles of 0° to 20° as measured from the nose tip, the temperature of the radome can be estimated as shown in Figures 13 and 14. 0° scan angle corresponds to the stagnation point temperature of 1400° F. 2° scan angle corresponds to a temperature of 1370° F and so forth (see Figures 13 and 14). This procedure can also be used to treat non-linear temperature distributions along the length of the radome. To model other temperature distribution with RTFRACP, these temperatures have to be converted into the proper dielectric constants and loss tangents using equations 2 and 3. Each scan angle which corresponds to an external point on the radome surface and, thus, to a certain temperature can be translated into the dielectric properties at that particular temperature. The knowledge of the dielectric properties at each scan angle allows for the calculation of the BSE at a particular scan angle. This allows for the construction of tables similar to Table 2. This table allows for the plotting of BSE versus scan angle such as Figures 15 and 16.

TEMPERATURE EFFECTS ON ELEVATION BSE - VS - SCAN ANGLE  
90° SCAN PLANE

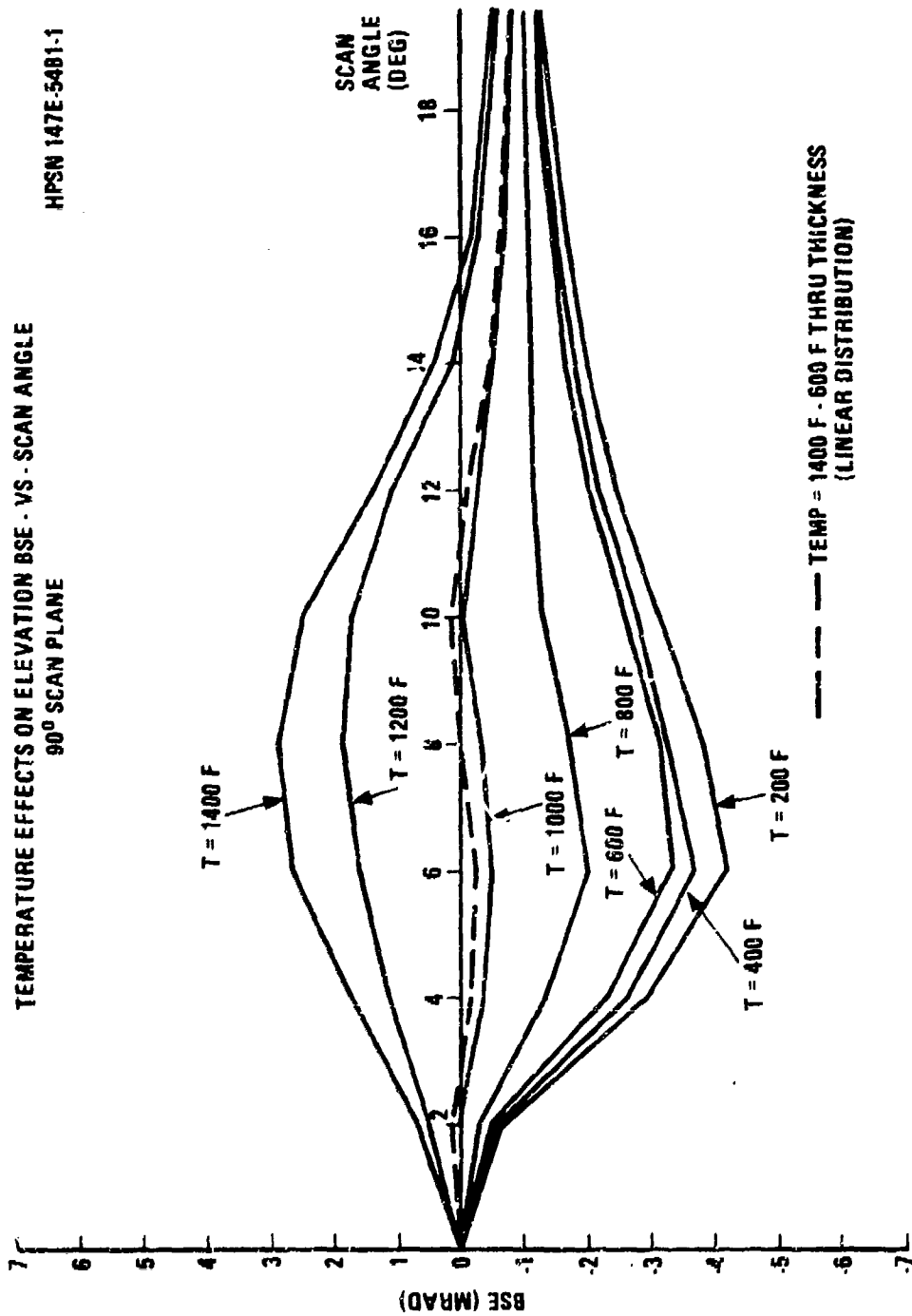


FIGURE 11. TEMPERATURE EFFECTS ON ELEVATION BSE - VS - SCAN ANGLE

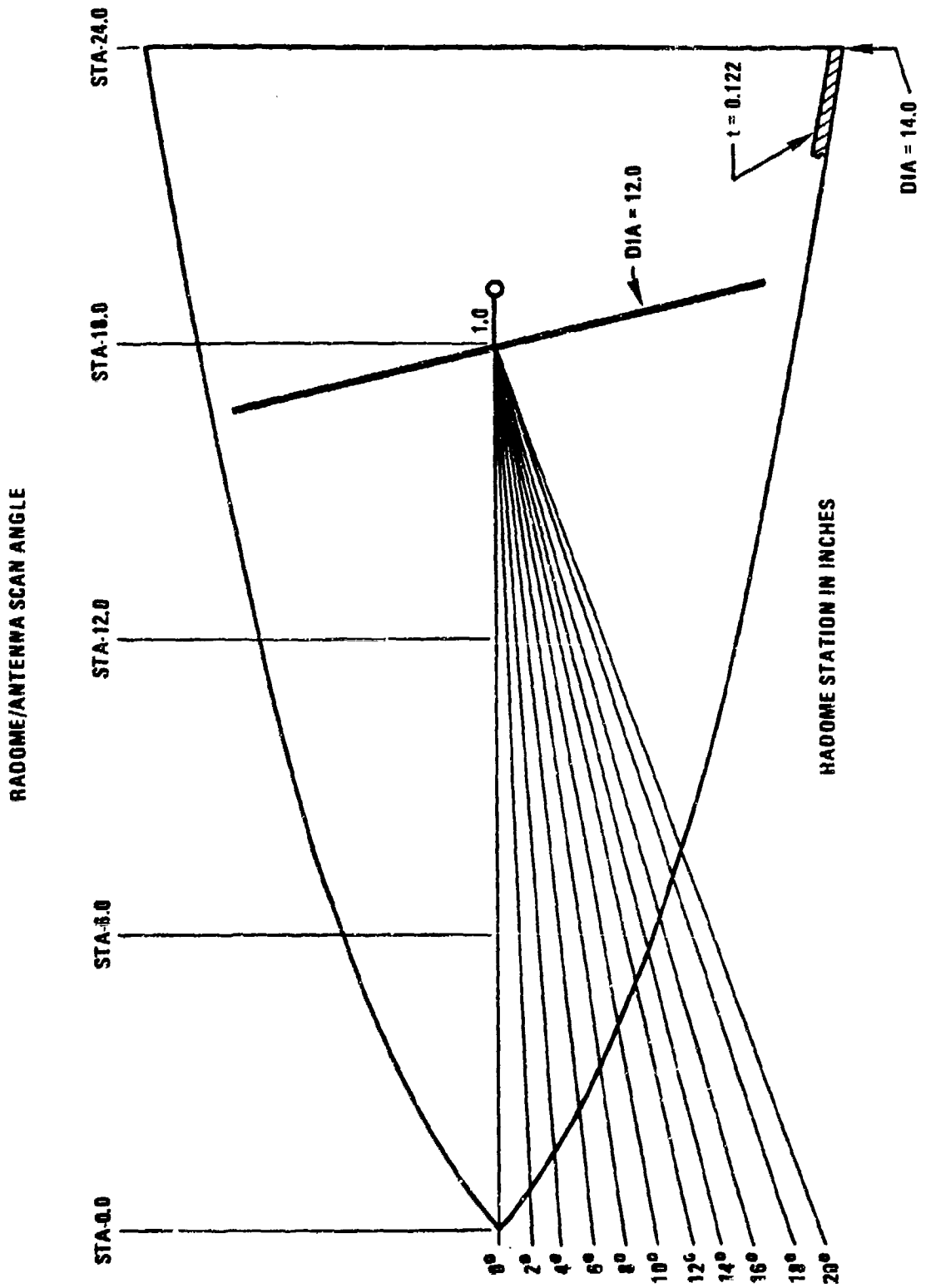


FIGURE 12. MODEL FOR DETERMINING TEMPERATURE AT 0° - 20° SCAN ANGLE

TYPICAL LINEAR TEMP PROFILE - VS - STATION

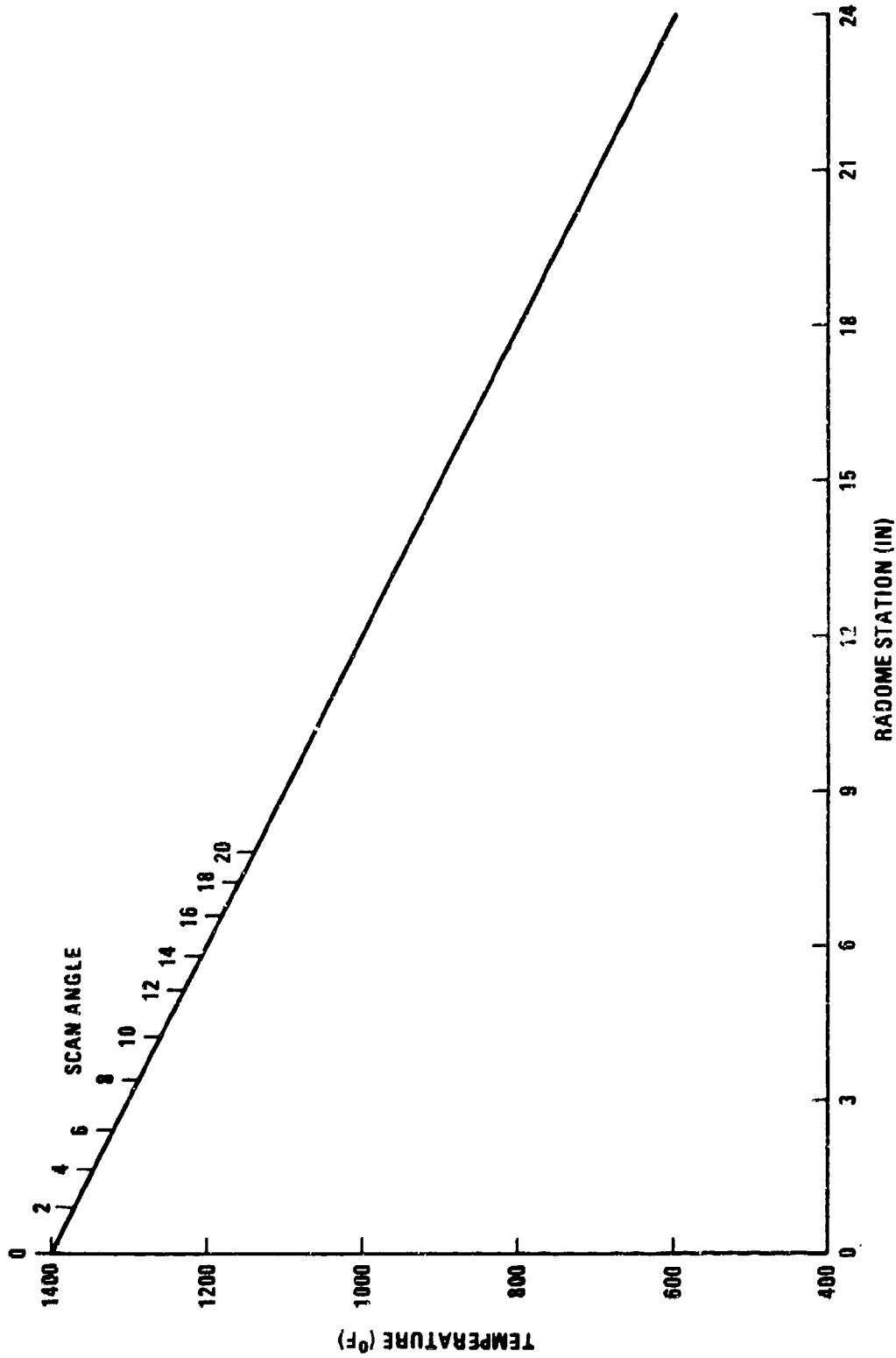


FIGURE 13. TEMPERATURE ALONG RADOME LENGTH

TEMPERATURE @ 0-20° SCAN ANGLES

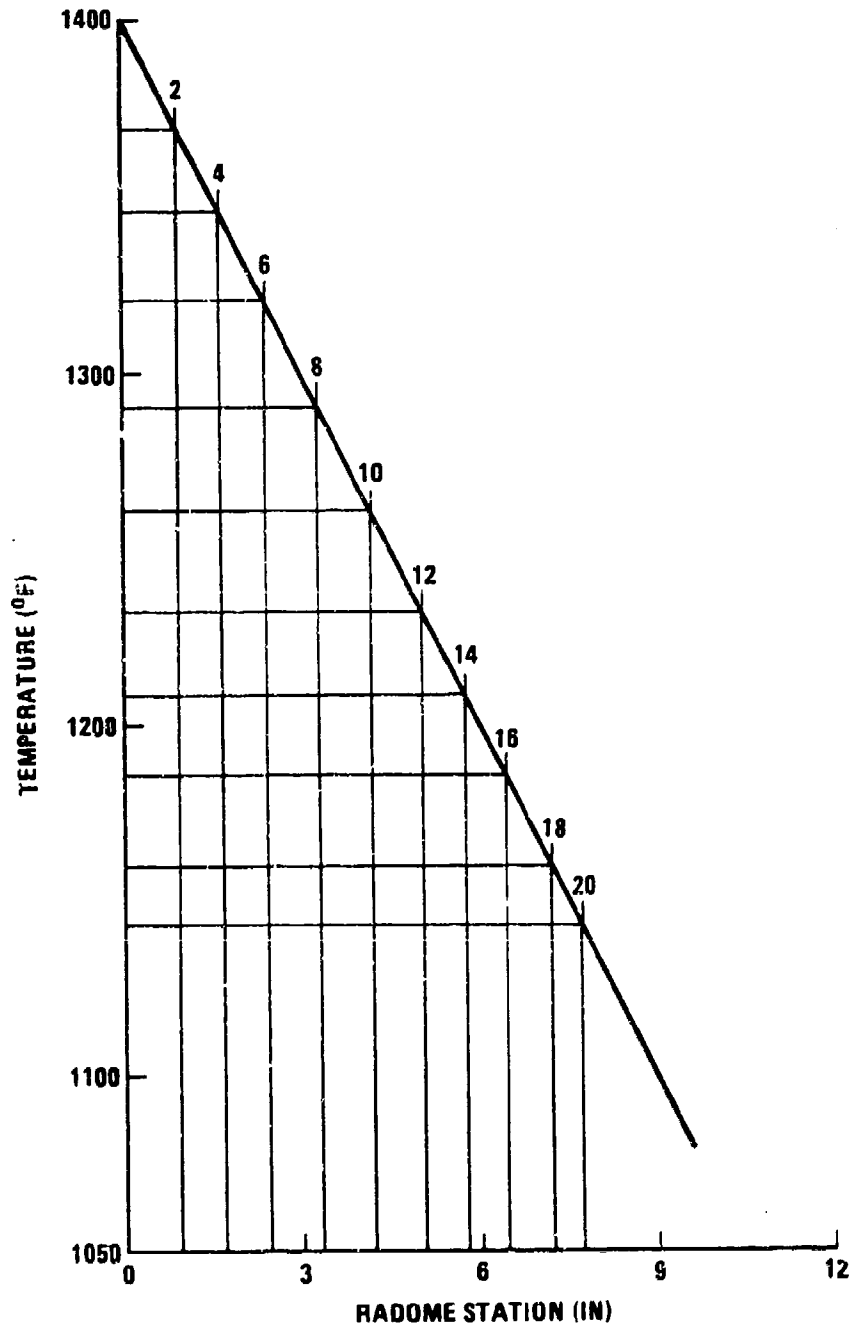


FIGURE 14. TEMPERATURE AT 0°- 20° SCAN ANGLE

TEMPERATURE EFFECTS ON AZIMUTH BSE - VS - SCAN ANGLE

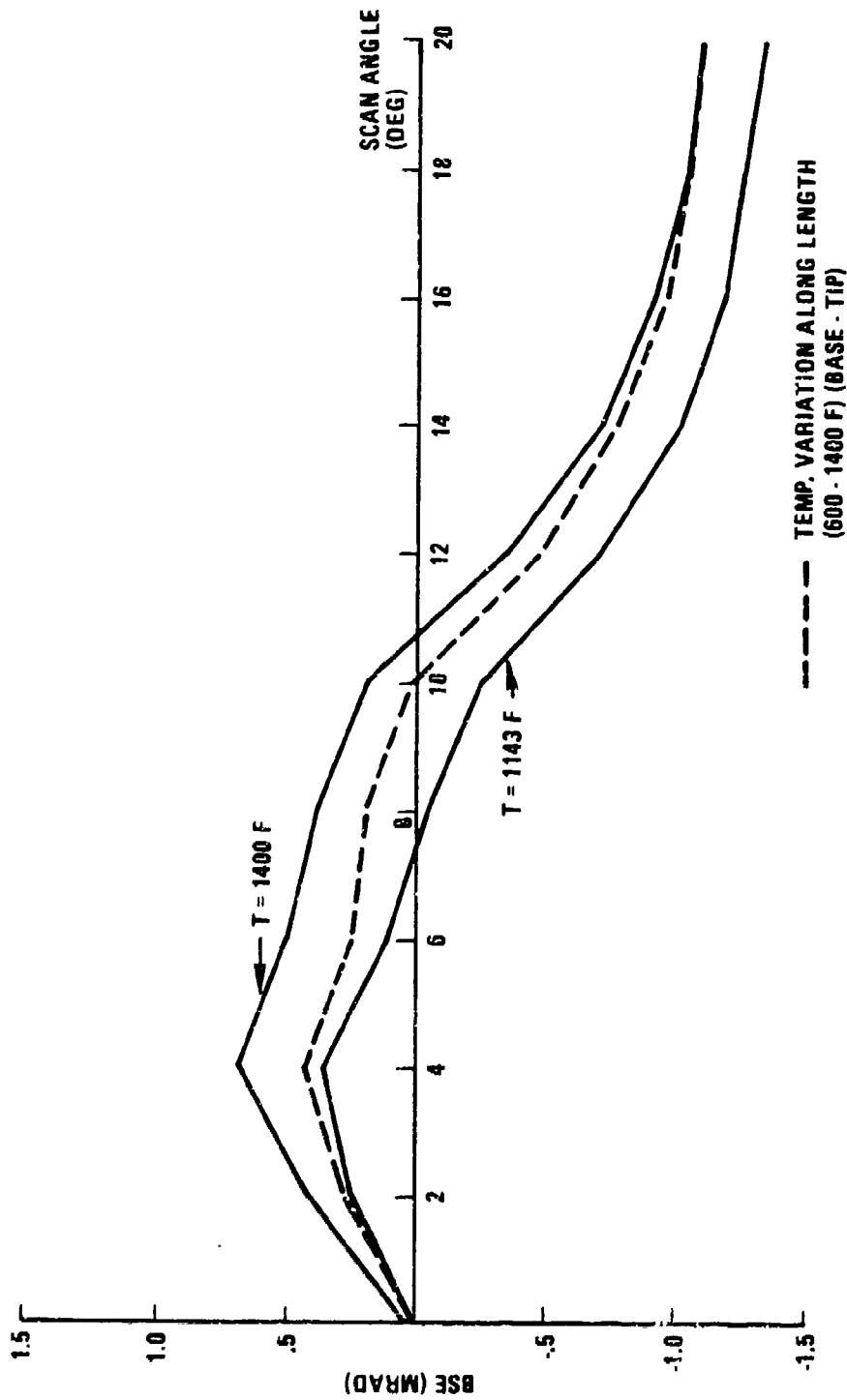


FIGURE 15. TEMPERATURE EFFECTS ON AZIMUTH BSE-VS-SCAN ANGLE

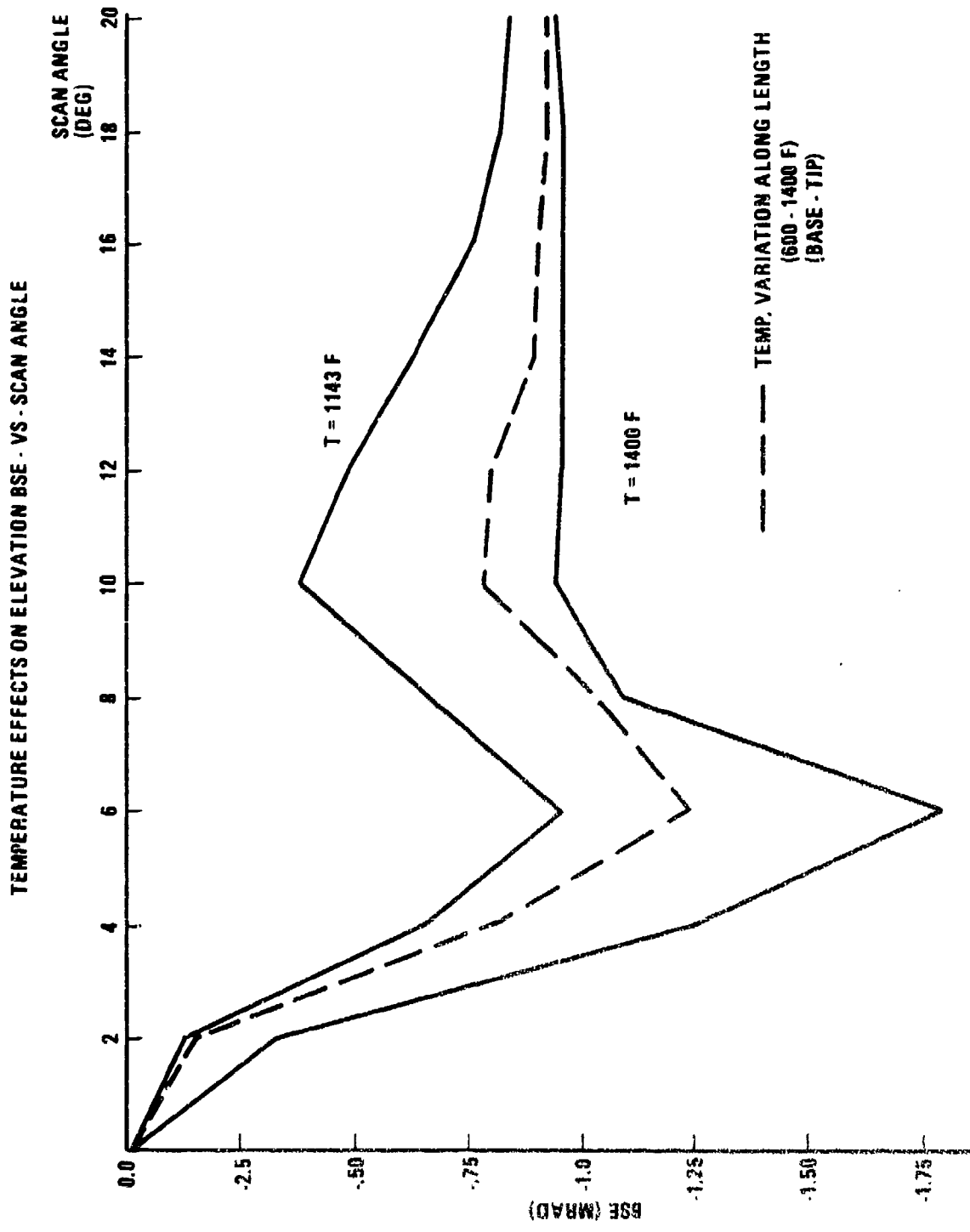


FIGURE 16. TEMPERATURE EFFECTS ON ELEVATION BSE-VS-SCAN ANGLE

TABLE 2. TEMPERATURE AND DIELECTRIC PROPERTIES AT 0° - 20° SCAN ANGLE

<u>SCAN ANGLE</u>	<u>TEMP(°F)</u>	<u>DIE CONST*</u>	<u>LOSS*</u>	<u>EL BSE</u>	<u>AZ BSE</u>
0	1400	8.489	0.009015	- .01	0
2	1370	8.482	0.008918	- .15	.27
4	1347	8.477	0.008846	- .80	.44
6	1321	8.471	0.008769	- 1.22	.25
8	1280	8.462	0.008653	- 1.07	.20
10	1262	8.458	0.008605	- .78	.03
12	1232	8.452	0.008527	- .80	- .45
14	1208	8.447	0.008468	- .89	- .78
16	1186	8.442	0.008415	- .92	- .96
18	1160	8.436	0.008356	- .95	- 1.05
20	1143	8.432	0.008319	- .94	- 1.10

\*Derived from equations 2 and 3.<sup>20</sup>

Figures 15 and 16 are plots of azimuthal and elevation BSE versus scan angles respectively. The middle curves represent the results of the analysis discussed above, i.e., a longitudinal temperature (600°F - 1400°F) variation along the length of the radome. The curves labeled 1400° F represent results assuming the entire radome is at a uniform temperature of 1400° F (stagnation point temperature). The lower curves represent results assuming the entire radome is at a uniform temperature of 1143° F (20° scan angle temperature, Table 2). Therefore, the 1400° F curves and the 1143° F curves represent bounding conditions for the case of the longitudinal temperature variation.

Figure 17 is a plot representing a change in BSE caused by flight through a rainfield whose effect is an increase in material erosion. This data is presented only as an illustration of how to treat BSE caused by material removal. Hot-pressed silicon nitride (HPSN) is used in this example. However, in actuality empirical data indicates that HPSN would show no erosion up to the point of catastrophic failure.<sup>21</sup> This is due to HPSN's low porosity. It was assumed for

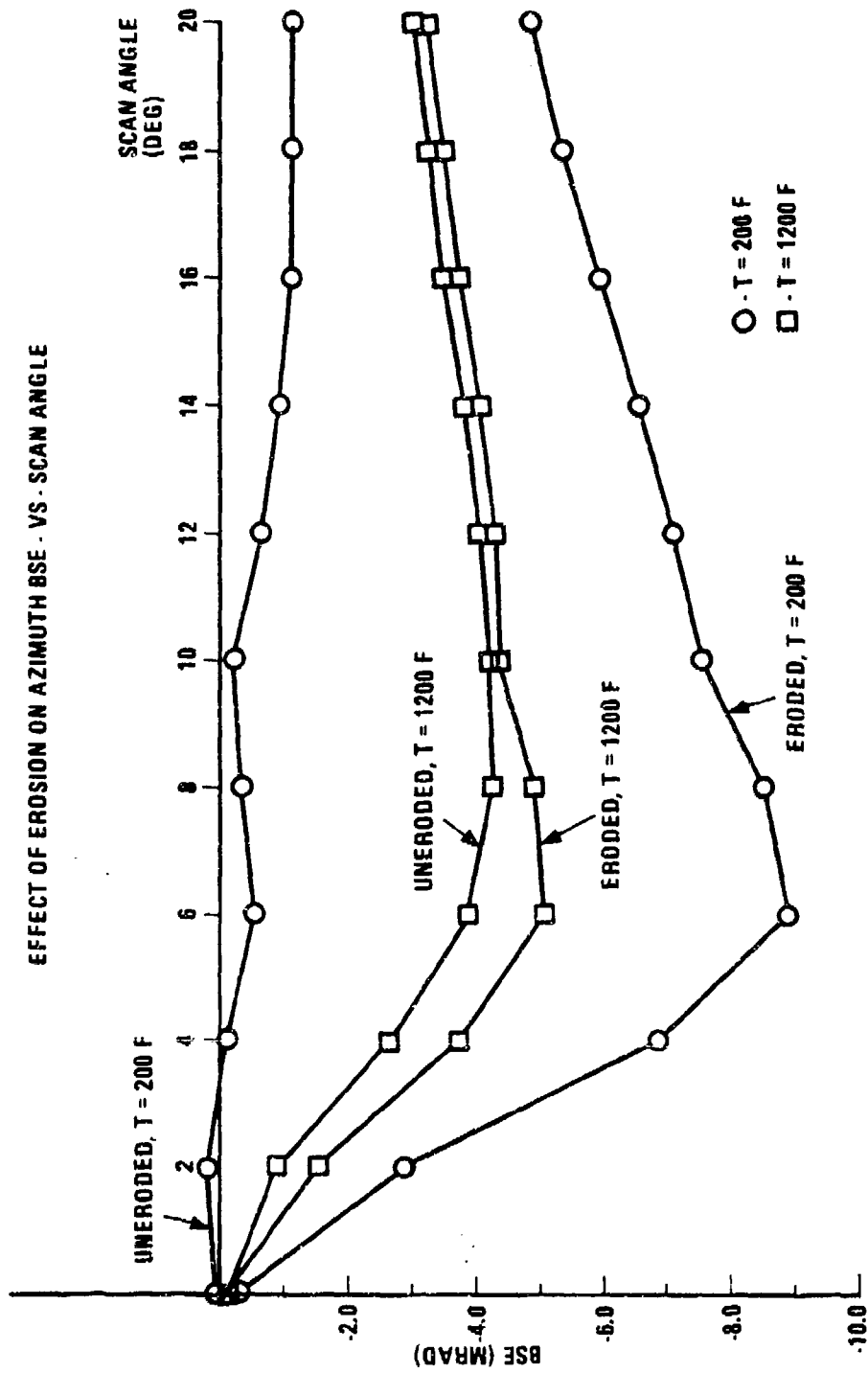


FIGURE 17. EFFECT OF EROSION ON AZIMUTH BSE-VS-SCAN ANGLE

this study that  $6.629 \times 10^{-3}$  inches of material was removed by erosion.<sup>20</sup> This amount of radome material removal is representative of a radome made from high porosity materials, such as slip casted fused silica (SCFS) flying at a velocity of 10 Kft/s through a rainfield of 20 mm/hr. HPSN is used in this calculation for the sake of consistency. Figure 17 shows the increase in azimuthal BSE caused by erosion at 2250° F. The plot shows that erosion has a greater effect on BSE at 200° F than at 1200° F.

Figures 18 and 19 show the effect of allowing the frequency to vary from 34.96 GHz to 35.05 GHz. Data is shown for 200° F and 2250° F radomes. The frequency variation results in an increase in BSE of less than one milliradian, while the temperature variation causes an increase in BSE of roughly 6 milliradians. Thus, the changes in BSE are dominated by temperature variation.

EFFECT OF FREQUENCY VARIATION ON AZIMUTHAL BSE VERSUS SCAN ANGLE

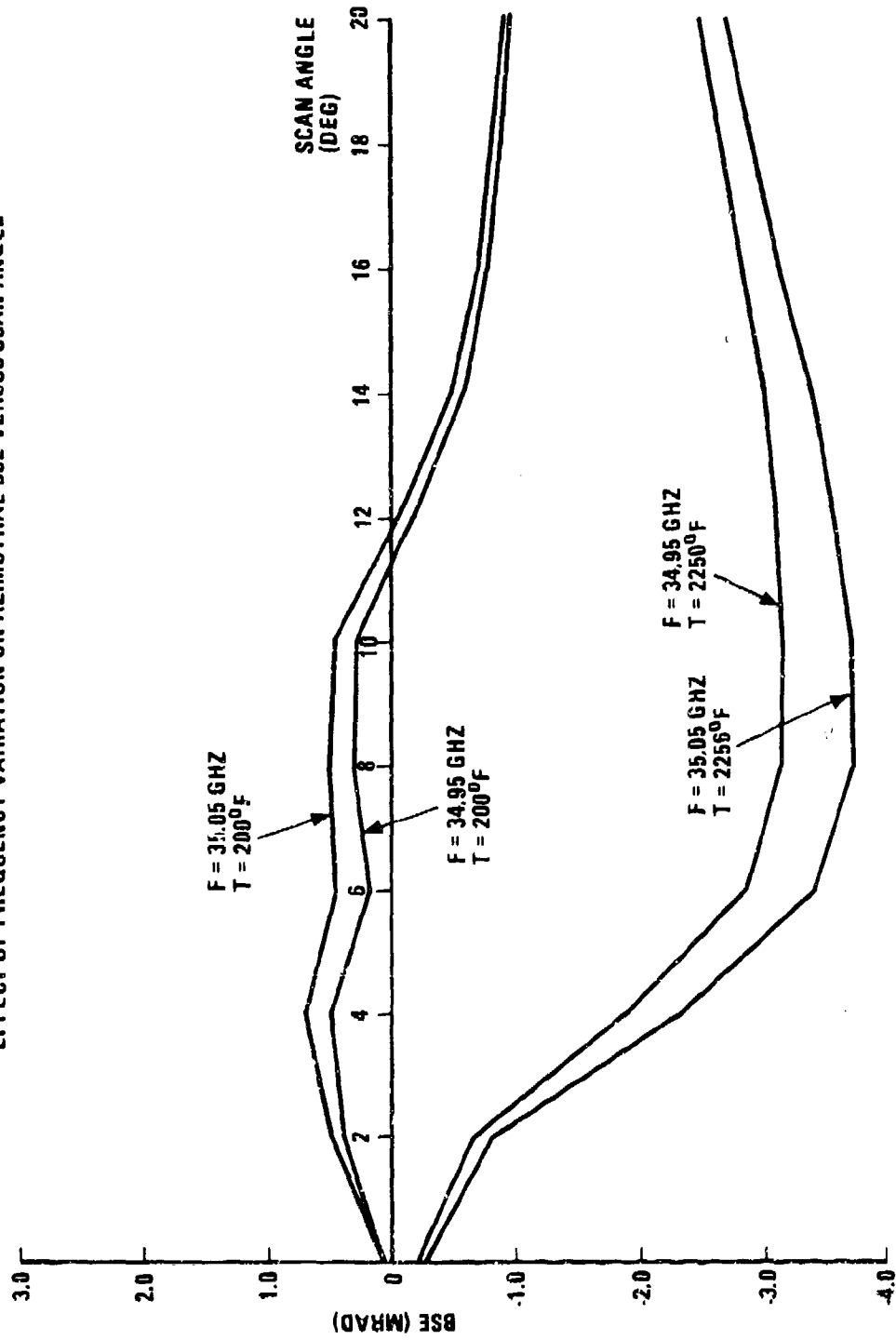


FIGURE 18. EFFECT OF FREQUENCY VARIATION ON AZIMUTH BSE-VS-SCAN ANGLE

EFFECT OF FREQUENCY VARIATION ON ELEVATION BSE VERSUS SCAN ANGLE

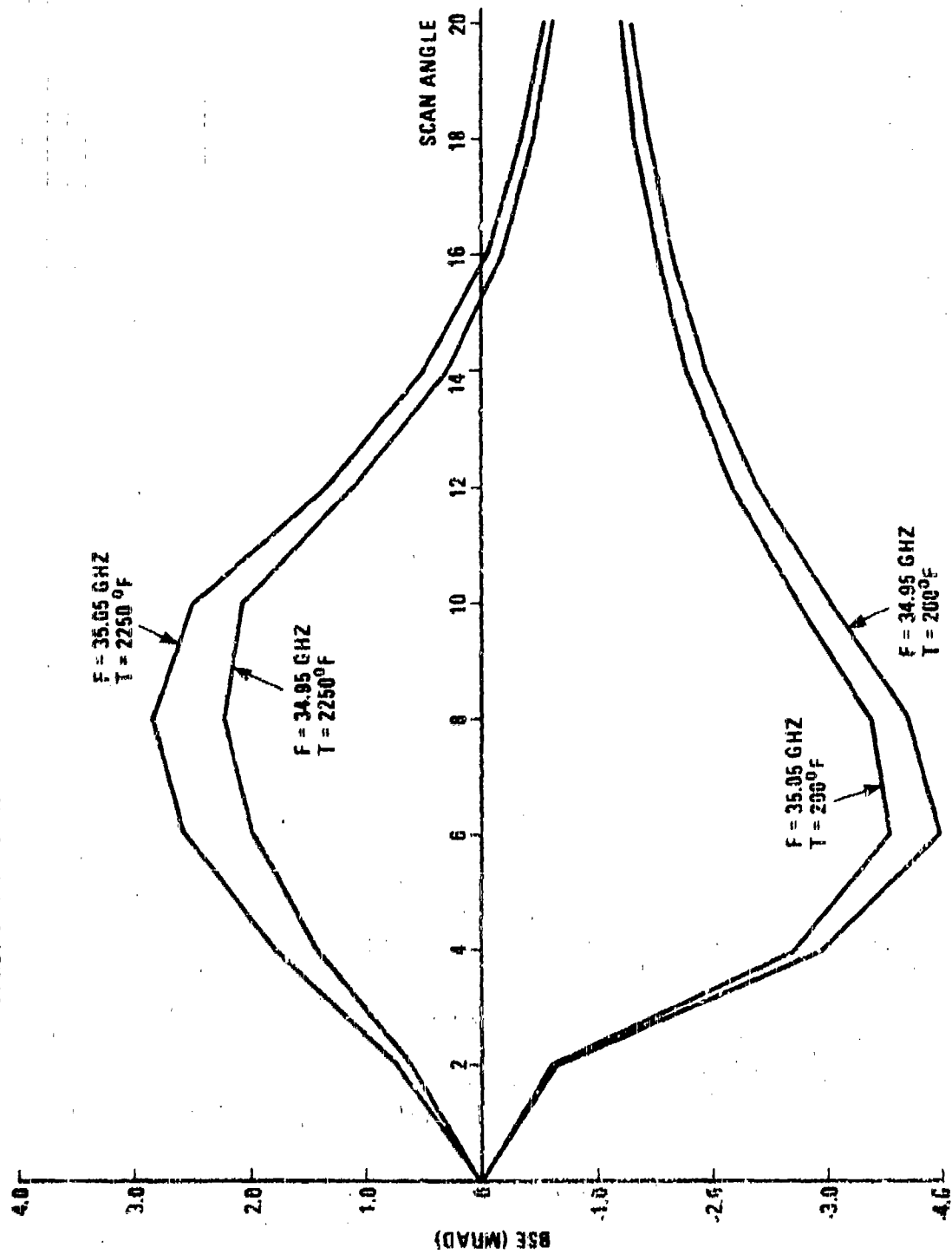


FIGURE 19. EFFECT OF FREQUENCY VARIATION OF ELEVATION BSE-VS-SCAN ANGLE

## 6. CONCLUSIONS AND RECOMMENDATIONS

It is quite obvious that RTFRACP is a useful tool with wide application in the area of radome/antenna evaluation. It should be emphasized that this study has not been exhaustive. Data has been presented to verify proper operation of the computer program and to show that Telodyne Brown Engineering has the knowledge and capability to apply this code to BMD systems. It should also be emphasized that the results of RTFRACP are not exact answers. No computer aided radome analysis programs give exact answers. This tool is useful in analyzing the impact of a design change or adverse environment on radome performance.

One main point is that the magnitude and the sign of BSE are very sensitive to radome temperature variations but are relatively insensitive to frequency variations in the millimeter wave regime. Another point is that through the use of such a code the amount of testing associated with both design changes and the environment can be greatly reduced. Thus, the use of the code is cost effective.

## 7. REFERENCES

1. Walton, J. D. Radome Engineering Handbook: Design and Principles, Marcel Dekker, Inc., 1970.
2. Bassett, H. L., et. al. "Radome and IRdome Technology," A Short Course of Instruction, U.S. Army Missile Command, November 15-17, 1982.
3. Silver, S. Microwave Antenna Theory and Design, McGraw-Hill, pp. 522-542, New York, 1949.
4. Kilcoyne, N. R. "An Approximate Calculation of Radome Boresight Error," Proc. USAF/Georgia Tech Symposium on Electromagnetic Windows, pp. 91-111, June 1968.
5. Van Doeren, R. E. "Application of an Integral Equation Method to Scattering from Dielectric Rings," Proc. USAF/Georgia Tech Symposium on Electromagnetic Windows, pp. 113-127, June 1968.
6. Tricoles, G. P. "Radiation Patterns and Boresight Error of a Microwave Antenna Enclosed in a Axially Symmetric Dielectric Shell," Journal of the Optical Society of America, 54, No. 9, pp. 1094-1101, September 1964.
7. Tavis, M. "A Three-Dimensional Ray Tracing Method for the Calculation of Radome Boresight Error and Antenna Pattern Distortion," Report No. TOR-0059 (56860)-2, Air Force Systems Command, May 1971.
8. Paris, D. T. "Computer-Aided Radome Analysis," IEEE Transaction, AP-18, No. 1, pp. 7-15, January 1970.
9. Wu, D. C. F., and Rudduck, R. C. "Plane Wave Spectrum-Surface Integration Technique for Radome Analysis," IEEE Transaction, AP-22, No. 3, pp. 497-500, May 1974.
10. Joy, E. B., and Huddleston, G. K. "Radome Effects on Ground Mapping Radar," Contract DAAH01-72-C-0598, U.S. Army Missile Command, AD-778 203/0, March 1973.

11. Chesnut, Robert. "LAMPS Radome Design," Proceedings of the 13th Symposium on Electromagnetic Windows, Georgia Institute of Technology, pp. 73-78, September 1976.
12. Huddleston, G.K., Bassett, H. L., and Newton, J. M. "Parametric Investigation of Radome Analysis Methods," 1978 IEEE AP-5 International Symposium Digest, pp. 199-201, May 1978.
13. Siwiak, K., Dowling, T., and Lewis, L.R. "The Reaction Approach to Radome Induced Boresight Error Analysis," America Optical Society, pp. 203-205.
14. Hayward, R. A., Rope, E. L., and Tricoles, G. P. "Accuracy of Two Methods for Numerical Analysis of Radome Electromagnetic Effects," Proceedings of the 14th Symposium on Electromagnetic Windows, Georgia Institute of Technology, pp. 53-55, June 1978.
15. Burks, D. G., Graf, E. R., and Fahey, M. D. "Effects of Incident Polarization on Radome-Induced Boresight Errors," Proceedings of the 15th Symposium on Electromagnetic Windows, Georgia Institute of Technology, pp. 1-5, June 1980.
16. Kvam, T. M. and Mei, K. K. "The Internal Fields of a Layered Radome Excited by a Plane Wave," 1981 IEEE AP-5 International Symposium, pp. 608-611, June 1981.
17. Huddleston, G. K., Bassett H. L., and Newton, J. M. "Parametric Investigation of Radome Analysis Methods; Computer Aided Radome Analysis Using Geometric and Lorentz Reciprocity," Final Technical Report AFOSR-77-3469, Vol. I, II, III, Georgia Institute of Technology, February 1981.
18. "Endo Homing Millimeter Wave Sensor Technology," OAB164, Prepared for U.S. Army BMD under Contract DASG60-77-C-0169, Martin Marietta Corp., Orlando, Florida, October 1978.
19. Ho, W. W. "High Temperature Millimeter Wave Characterization of the Dielectric Properties of Advanced Window Materials," AMMRC TRS2-28, U.S. Army Materials and Mechanics Research Center, Watertown, MA, May 1982,

20. Kozakoff, D. J. "Environmental Effects on Radomes." Final Report 82016, August 1982.
21. Letson, K. N. and Burleson, W. G. "Final Evaluation of Rain Erosion Sled Test Results at Mac 3.7 to 5.0 for SCFS Radome Structures," Technical Report T-79-42, U.S. Army Missile Command, Redstone Arsenal, Alabama, March 1979.

## Distribution List

### Department of the Army

#### Ballistic Missile Defense Command

ATTN: L. Atha, BMDATC-RN

ATTN: R. Buckelew, BMDSC-HEDS

ATTN: J. Butler, BMDATC-RN

ATTN: F. Kendall, BMDSC-HEDS

ATTN: S. Massey, BMDATC-RN

### Department of Defense Contractors

#### Teledyne Brown Engineering

ATTN: C. Boles

ATTN: F. Leopard

ATTN: J. Mullins

ATTN: T. Reiman

ATTN: R. Wells

### Defense Technical Information Center

ATTN: DD